Macrocyclic receptor showing improved Pb^{II}/Zn^{II} and Pb^{II}/Ca^{II} selectivities[i]

Raquel Ferreirós-Martínez, Carlos Platas-Iglesias, Andrés de Blas, David Esteban-Gómez* and Teresa Rodríguez-Blas†

Departamento de Química Fundamental, Universidade da Coruña, Alejandro de la Sota 1, 15008 A Coruña, Spain

European Journal of Inorganic Chemistry, volume 2010, issue 17, pages 2495–2503, June 2010
Received 17 December 2009, version of record online 06 May 2010, issue online 31 May 2010

Abstract

Herein we report on the macrocyclic receptor *N*,*N*′-bis[(6-carboxy-2-pyridyl)methyl]-1,10-diaza-15-crown-5 (**H_2bp15c5**) and its coordination properties towards Zn^{II}, Cd^{II}, Pb^{II}, and Ca^{II}. The stability constants of these complexes determined by pH-potentiometric titration at 25 °C in 0.1 M KNO_3 vary in the following order: $Pb^{II} > Cd^{II} >> Zn^{II} > Ca^{II}$. As a result, **bp15c5** presents very important Pb^{II}/Zn^{II} and Pb^{II}/Ca^{II} selectivities. These results are in contrast to those reported for the related receptor derived from 1,7-diaza-12-crown-4, which provides very similar complex stabilities for Zn^{II} and Pb^{II}. The X-ray crystal structure of [Cd(**Hbp15c5**)]$^+$ shows heptadentate binding of the ligand to the metal ion, with two oxygen atoms of the macrocyclic unit remaining uncoordinated. The ^{1}H NMR spectra of the complexes formed with Pb^{II}, Zn^{II}, and Ca^{II} (D_2O) show very broad peaks in the region 2–5 ppm, indicating an important degree of flexibility of the crownmoiety in these complexes. On the contrary, the ^{1}H and ^{13}C NMR spectra recorded for the Cd^{II} complex are well resolved and could be fully assigned. A detailed conformational investigation using theoretical calculations performed at the DFT (B3LYP) level predict a minimum energy conformation for [Cd(**bp15c5**)] that is very similar to that observed in the solid state. Analogous calculations performed on the [M(**bp15c5**)] (M = Zn or Pb) systems predict hexadentate binding of the ligand to these metal ions. In the case of the Pb^{II} complex our calculations indicate that the 6s lone pair is stereochemically active, which results in a hemidirected coordination geometry around the metal ion. The minimum energy conformations calculated for the Zn^{II}, Cd^{II}, and Pb^{II} complexes are compatible with the experimental NMR spectra obtained in D_2O solution.

Keywords: macrocycles; selectivity; lead; cadmium; crown compounds

* david.esteban@udc.es
† teresa.rodriguez.blas@udc.es

Introduction

Selective complexation of metal ions is of fundamental importance in broad areas of both chemistry and biochemistry. Among the different platforms used for metal-ion discrimination, macrocyclic receptors such as crown ethers,[1] calixarenes,[2] or cryptands[3] play an essential role. These receptors possess a high level of preorganization that often results in superior selectivities of their complexes with metal ions in comparison to those of acyclic ligands. Particularly interesting are the studies reported by R. D. Hancock concerning the factors that control the metal-ion binding affinity, especially those related to the metal-ion complementarity of ligand architectures.[4,5] In the case of macrocyclic ligands, three major strategies emerge for achieving effective complexation:[6,7] (i) the use of donor set variation to tune the affinity of the receptor towards particular metal ions; (ii) the hole-size effect, that is, the use of ring size variation to maximize the thermodynamic stability of the complex by matching the radius of the metal ion to the hole size of the macrocyclic moiety; and (iii) the use of substituent variation to take advantage of the effect of pendant arms to the donor atoms of the parent macrocycle on metal-ion discrimination.

The interest in the coordination chemistry of cadmium(II) and lead(II) in aqueous solution is related to their inherent toxicity and health effects and to the widespread industrial uses of their compounds.[8,9] Lead poisoning particularly affects young children who can absorb up to 50 % of ingested lead.[10] Once ingested through the gastrointestinal tract, lead accumulates in soft tissues including vital organs such as the kidneys, liver, or brain, where it is bound to thiol and phosphate groups in proteins, nucleic acids, and cell membranes[11,12] causing severe neurological and/or hematological effects.[13] Damage to the lung in workers exposed to cadmium was the first human health effect related to cadmium in a report published already 70 years ago.[14] Exposure to Cd^{II} causes bone diseases, gastrointestinal and renal dysfunction, and cadmium and cadmium compounds are regarded as carcinogenic to humans.

In previous papers we have reported on the complexation properties of the macrocyclic ligand containing picolinate pendants **bp12c4** (Scheme **1**) toward divalent metal ions such as Ca^{II}, Zn^{II}, Cd^{II}, and Pb^{II},[15] and trivalent lanthanide ions.[16] We have shown that **bp12c4** forms stable complexes with Zn^{II}, Cd^{II}, and Pb^{II} in aqueous solution, but it does not show important selectivity for any of these three metal ions. As a continuation of these works, herein we report the new ligand **bp15c5**, which possesses a larger crown moiety. This structural modification, together with the presence of neutral oxygen atoms in the crown moiety,[5] is expected to provide a certain degree of selectivity for large metal ions such as Pb^{II} over Zn^{II} and Ca^{II}. Thus, the stability of the complexes of **bp15c5** formed with Ca^{II}, Zn^{II}, Cd^{II}, and Pb^{II} was studied by pH-potentiometric titrations. The structure of the complexes in solution was investigated by ^{1}H and ^{13}C NMR spectroscopy and density functional theory calculations performed at the B3LYP level. Finally, the single-crystal X-ray structure of the Cd^{II} complex is also reported.

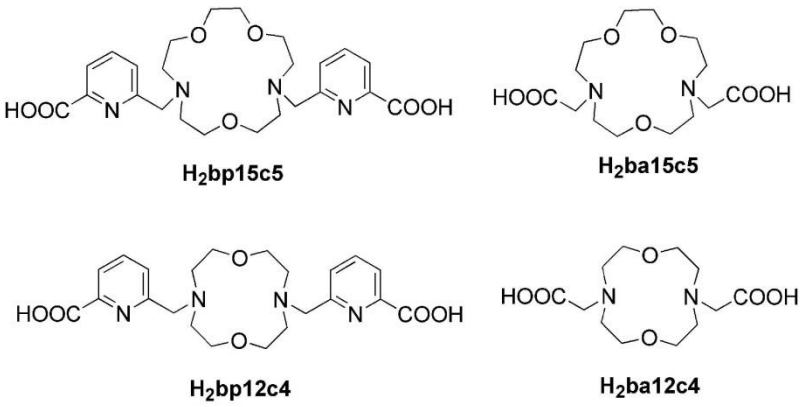

Scheme 1. Ligands discussed in the present work.

Results and discussion

Synthesis of bp15c5

Ligand **H_2bp15c5** (Scheme **1**) was obtained by using a *N*-alkylation reaction of 1,10-diaza-15-crown-5 with methyl 6-(chloromethyl)pyridine-2-carboxylate in refluxing acetonitrile in the presence of Na_2CO_3, followed by deprotection of the methyl esters of the intermediate with 6 M HCl.

Ligand protonation constants and stability constants of the metal complexes

The protonation constants of **bp15c5** as well as the stability constants of its metal complexes formed with Ca^{II}, Zn^{II}, Cd^{II}, and Pb^{II} were determined by potentiometric titration in 0.1 M KNO_3; the constants and standard deviations are given in Table **1**, which also lists the protonation and stability constants reported for the related systems **bp12c4**,[15] **ba15c5**[17], and **ba12c4**[18] (Scheme **1**). The experimental titration curves are shown in Figure **1**. The ligand protonation constants are defined as in Equation (**1**), and the stability constants of the metal chelates and the protonation constants of the complexes are expressed in Equations (**2**) and (**3**), respectively.

$$K_i = \frac{[H_iL]}{[H_{i-1}L][H^+]} \quad (1)$$

$$K_{ML} = \frac{[ML]}{[M][L]} \quad (2)$$

$$K_{MH_iL} = \frac{[MH_iL]}{[MH_{i-1}L][H^+]} \quad (3)$$

In comparison to the bisacetate derivative of the same macrocycle (**ba15c5**, Scheme **1**), **bp15c5** has lower protonation constants for the first and second protonation steps, which occur on the amine nitrogen atoms. This is in line with previous investigations, which showed that the replacement of the carboxylate groups of EDTA by pyridinecarboxylate units leads to a decrease in the basicity of the two amine nitrogen atoms.[19] The protonation constant obtained for the first protonation step of **bp15c5** is slightly lower than that reported for **bp12c4**; a similar situation is observed when comparing the $\log K_1$ values of the bisacetate derivatives **ba12c4** and **ba12c5**. However, the protonation constants determined for the second protonation step are slightly higher in the case of the ligands derived from diaza-15-crown-5 than in those based on 12-crown-4. This is attributed to a lower electrostatic repulsion between the two protonated amine nitrogen atoms in the ligands derived from the largest crown moiety as a consequence of their relatively large separation. This result is in line with the higher $\log K_2$ value observed for DTPA when compared to EDTA; the second $\log K_i$ in DTPA corresponds to the protonation of one of the terminal nitrogen atoms, with displacement of the first proton from the central to the other terminal nitrogen atom.[20] The last two protonation steps in **bp15c5**, which are very similar to those obtained for **bp12c4**, are attributed to the protonation of the pyridylcarboxylate groups.[21,22]

Potentiometric titrations of **H_2bp15c5** were carried out in the presence of equimolar Ca^{II}, Zn^{II}, Cd^{II}, and Pb^{II} ions in order to determine the stability constants of the corresponding metal complexes (Table **1**). The

1:1 titration curves with all metal ions display an inflection at $a = 2$ [a = mol of OH^-/mol of ligand], as expected for the formation of [M(**bp15c5**)] species (M = Ca, Zn, Cd, or Pb). The **bp15c5** complex of Pb^{II} shows the highest $\log K_{ML}$ value among the different divalent metal ions studied in this work. The $\log K_{PbL}$ value obtained for **bp15c5** is ca. 4.3 $\log K$ units higher than that reported for ba15c5, and slightly higher than that determined previously for **bp12c4**. The $\log K_{ML}$ values obtained for the Ca^{II}, Zn^{II}, Cd^{II} complexes of **bp15c5** are lower than those obtained for **bp12c4**, a particularly low stability constant being observed for the Zn^{II} complex.

Table 1. Ligand protonation constants and thermodynamic stability constants of **bp15c5** and its metal complexes as determined by pH-potentiometry [I = 0.1 M KNO_3]. Data reported previously for **bp12c4**, **ba15c5**, and **ba12c4** are provided for comparison.

	bp15c5	**bp12c4**[a]	**ba15c5**[b]	**ba12c4**[c]
$\log K_1$	8.21(1)	8.67	9.02	9.53
$\log K_2$	7.19(1)	6.90	8.79	7.46
$\log K_3$	3.43(2)	3.42	2.95	2.11
$\log K_4$	2.53(1)	1.67		
$\log K_{ZnL}$	11.14(1)	15.48	14.08	12.28
$\log K_{ZnHL}$	4.33(1)	2.31		
$\log K_{CdL}$	15.84(1)	16.84	12.95	14.09
$\log K_{CdHL}$	2.62(10)			
$\log K_{PbL}$	17.17(1)	15.44	12.91	12.43
$\log K_{PbHL}$	2.52(6)	2.52		
$\log K_{CaL}$	9.12(3)	10.70	8.74	8.50
$\log K_{CaHL}$	5.04(1)	3.76		
$\log K_{CaH2L}$	4.60(1)			

[a] Ref.[15] [b] Ref.[17] [c] Ref.[18]

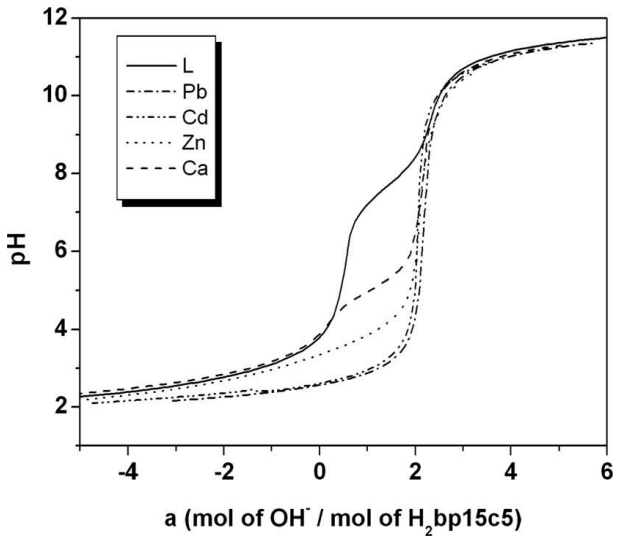

Figure 1. Titration curves of **H_2bp15c5** in the presence and absence of equimolar Ca^{II}, Zn^{II}, Cd^{II}, and Pb^{II} [I = 0.1 M (KNO_3), 25 °C].

The species distribution diagrams calculated for the complexes of **bp15c5** studied in this work are depicted in Figure **2**. Protonated forms of the complexes have been detected over the pH range studied for all complexes. Particularly high protonation constants have been obtained for the Zn^{II} and Ca^{II} complexes. The diagram obtained for Zn^{II} shows the formation of monoprotonated species at pH < 6.5, while for the Ca^{II} complex the protonated forms of the complex are observed already at pH < 7. In the case of Pb^{II} and Cd^{II} complexes the formation of protonated forms of the complexes are observed at lower pH values (<4.5). The speciation diagrams shown in Figure **2** highlight the selectivity of **bp15c5** for Pb^{II} over Zn^{II} and Ca^{II}. For instance, Pb^{II} is almost totally complexed at pH 3.0 (99.2 %), while only 18.0 % of the total Zn^{II} and 27.1 % of the total Ca^{II} are complexed under the same conditions. A certain selectivity for Pb^{II} over Cd^{II} is also observed, the total amount of Cd^{II} complexed at pH 3.0 being 96.6 %.

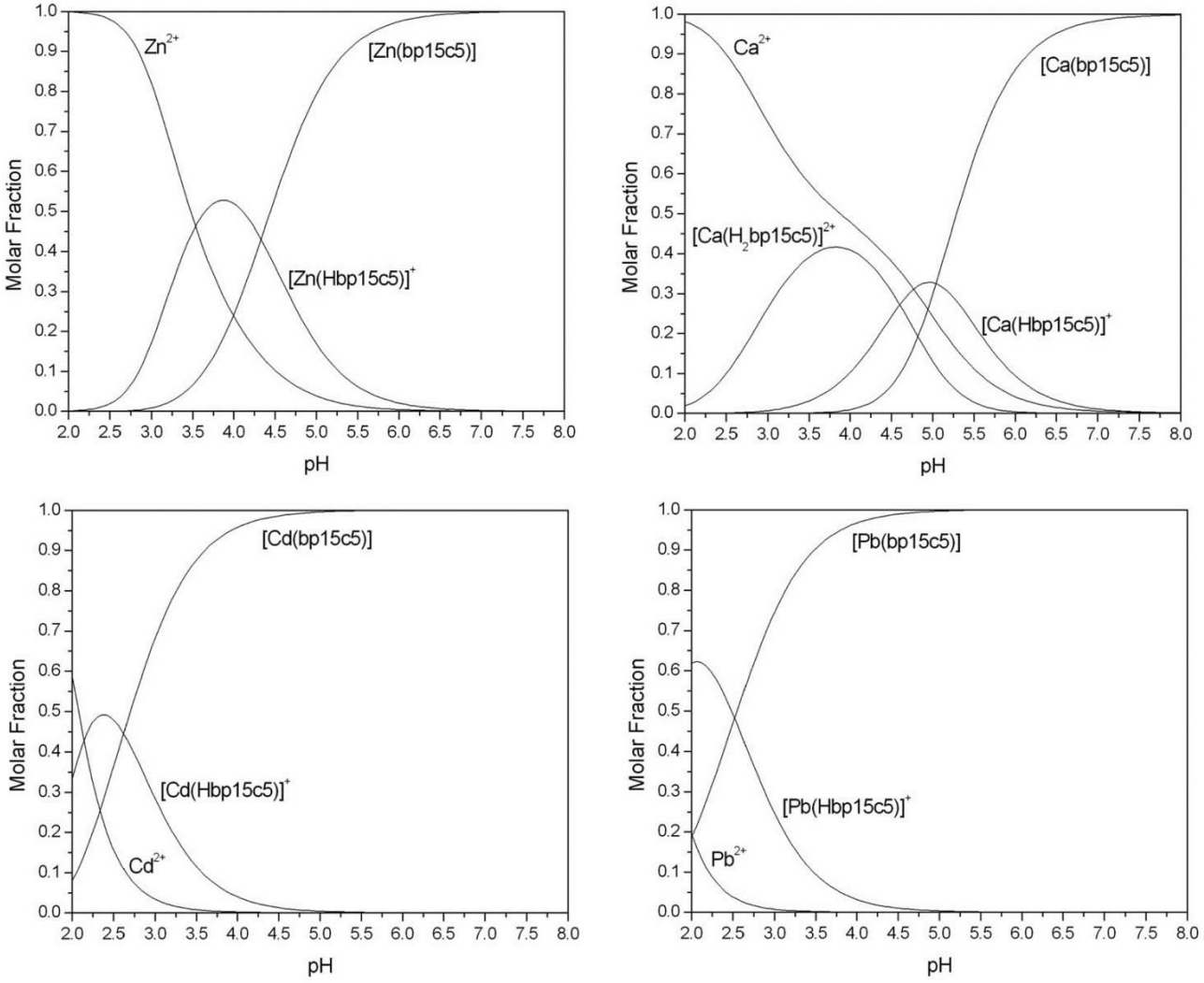

Figure 2. Species distribution of the M(**bp15c5**) systems (M = Zn, Ca, Pb, or Cd), 1:1 M:L; $[M^{II}]$ = 1 mM, μ = 0.1 M (KNO_3), 25 °C.

The thermodynamic stability constants alone are not sufficient to compare different complex stabilities under physiological conditions. Moreover, the comparison of stability constants of complexes with different stoichiometry is meaningless. The conditional stability constants, or more frequently the *p*M values, are considered to give a more realistic picture of complex stability. The *p*M values are usually defined as shown below.[23]

$pM = -\log [M]_{free}$ at pH = 7.4 for $[M^{II}]$ = 1 μM, [L] = 10 μM

The *p*M values obtained under these conditions for **bp15c5** complexes are compared to those of **bp12c4**, **ba12c4**, and **ba15c5** complexes in Table **2**. The stability of the Cd^{II}, Pb^{II}, and Ca^{II} complexes of **bp12c4** and **bp15c5** is clearly higher than that observed for the respective complexes of **ba12c4** and **ba15c5**. This is attributed to the higher denticity of the ligands containing picolinate groups, which favors the complexation of these relatively large metal ions. A comparison of the *p*M values calculated for **bp12c4** and **bp15c5** complexes shows that increasing the size of the crown moiety improves the stability of the complex formed with Pb^{II}, while the stability of the Zn^{II} complex decreases dramatically. In the case of Cd^{II} and Ca^{II} increasing the size of the crown fragment slightly decreases complex stability. As a result, **bp15c5** presents very important Pb^{II}/Zn^{II} and Pb^{II}/Ca^{II} selectivities. The stabilities of the complexes of **bp15c5** follow the trend $Pb^{II} > Cd^{II} >> Zn^{II} > Ca^{II}$. This is in contrast to the trend observed for the complexes of **ba12c4**, for which the Zn^{II} and Pb^{II} complexes possess very similar stabilities.

Table 2. Comparison of the *p*M values calculated for **bp15c5** complexes and related systems.[a]

	bp15c5	**bp12c4**	**ba15c5**	**ba12c4**
Zn	11.0	15.0	12.0	10.8
Cd	15.7	16.4	10.9	12.6
Pb	17.1	15.0	10.8	10.9
Ca	9.0	10.2	6.8	7.0

[a] $pM = -\log [M]_{free}$ at pH = 7.4 for $[M^{II}]$ = 1 μM, [L] = 10 μM.

Structural studies

The ^{1}H and ^{13}C NMR spectra of [M(**bp15c5**)] complexes were recorded in D_2O solution at pD = 7.0. The ^{1}H NMR spectra of the Ca^{II}, Zn^{II}, and Pb^{II} complexes show very broad peaks in the region 2–5 ppm at room temperature. Lowering the temperature to 278 K in D_2O or to 198 K in CD_3OD does not result in better resolved spectra (Supporting Information). However, the spectrum obtained for the Cd^{II} analogue at room temperature is well resolved, and therefore could be fully assigned (Table **3**, Figure **3**). The assignments of the proton signals were based upon HMQC and HMBC 2D heteronuclear experiments as well as standard 2D homonuclear COSY experiments, which gave strong cross-peaks between the geminal CH_2 protons (7–18) and between the *ortho*-coupled pyridyl protons. Although the specific CH_2 proton assignments of the axial and equatorial H7–H18 protons were not possible on the basis of the 2D NMR spectra, they were carried out using the stereochemically dependent proton shift effects, resulting from the polarization of the C–H bonds by the electric-field effect caused by the cation charge.[24] This results in a deshielding of the equatorial protons which are pointing away from the metal ion. The signals due to protons H7a, H7b, H18a, and H18b show AB spin patterns where the larger shifts for H7b and H18b result from the combined deshielding effects of the pyridyl ring current and the polarizing effect of the M^{II} ion on the C–H bond pointing away from it. The two picolinate pendant arms are magnetically nonequivalent, which results in a C_1 symmetry of the complex in solution. This is confirmed by the ^{13}C NMR spectrum, which shows 24 signals for the 24 carbon nuclei of the ligand backbone. These results indicate a slow interconversion between the Δ and Λ optical isomers arising from the different orientation of the two pendant arms (see below).

Table 3. ^{1}H and ^{13}C NMR shifts (ppm with respect to TMS) of [Cd(**bp15c5**)] recorded in D_2O solution (pD = 7.0) at 298 K.[a]

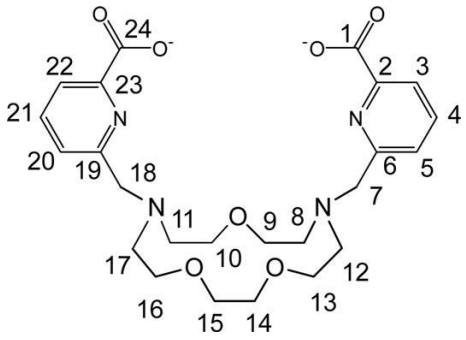

H3	7.90	H13ax	3.14	C1	170.7	C16	67.4
H4	8.03	H13eq	3.30	C2	149.6	C17	56.1
H5	7.61	H14ax	2.80	C3	124.6	C18	59.9
H7a	3.95	H14eq	3.38	C4	142.7	C19	156.6
H7b	4.60	H15ax	3.33	C5	124.7	C20	124.8
H8ax	2.95	H15eq	3.38	C6	157.3	C21	141.6
H8eq	3.61	H16ax	4.14	C7	62.2	C22	124.2
H9ax	3.71	H16eq	3.50	C8	59.8	C23	152.0
H9eq	3.92	H17ax	2.78	C9	67.5	C24	172.3
H10ax	3.49	H17eq	3.36	C10	67.1		
H10eq	3.87	H18a	3.71	C11	57.1		
H11ax	2.66	H18b	4.70	C12	57.2		
H11eq	2.98	H20	7.51	C13	66.9		
H12ax	2.36	H21	7.94	C14	69.9		
H12eq	3.47	H22	7.67	C15	70.7		

[a] $^{3}J_{5,4}$ = 7.8 Hz; $^{3}J_{20,21}$ = 7.8 Hz; $^{3}J_{22,21}$ = 7.6 Hz; $^{2}J_{7a,7b} = {}^{2}J_{7b,7a}$ = 16.3 Hz; $^{2}J_{18a,18b}$ = 16.2 Hz.

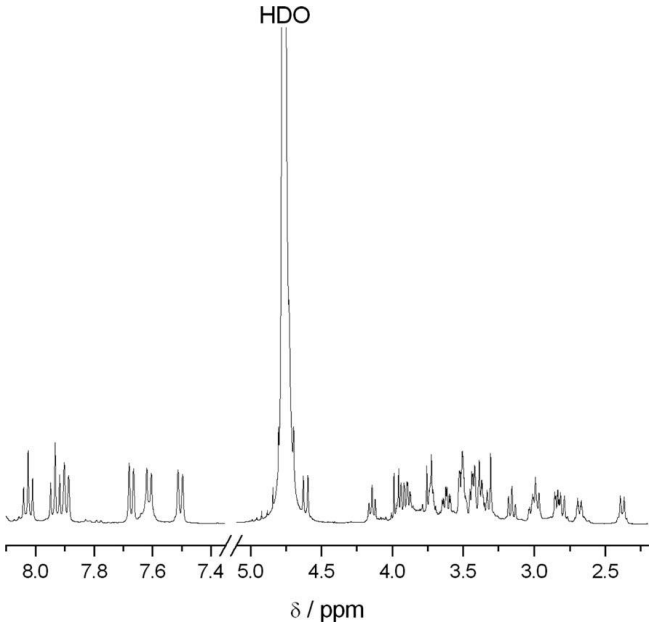

Figure 3. ^{1}H NMR spectrum of [Cd(**bp15c5**)] recorded in D_2O solution (pD = 7.0) at 298 K.

Crystals of formula [Cd(**Hbp15c5**)](ClO_4)·0.5H_2O have been obtained from the reaction in 2-propanol of **H_2bp15c5**·3HCl·3H_2O with Cd(ClO_4)$_2$·6H_2O in the presence of triethylamine. The carbon and oxygen atoms of the crown moiety are heavily disordered, the occupation factor of the positions with the highest occupation being 0.527(5). Figure **4** shows a view of the structure of the [Cd(**Hbp15c5**)]$^+$ complex, while bond lengths and angles of the metal coordination environment are shown in Table **4**. The metal ion is seven-coordinate by the donor atoms of the two picolinate pendants [N(1), O(1), N(4), and O(6)], the two pivotal nitrogen atoms [N(2) and N(3)] and one of the oxygen atoms of the crown moiety [O(5)]. The other two oxygen atoms of the crown fragment, O(3) and O(4), remain uncoordinated [Cd(1)–O(3) 3.225 Å, Cd(1)–O(4) 3.087 Å]. The complex is protonated on one of the oxygen atoms of a carboxylate group [O(7), see Figure **4**]. However, protonation of this picolinate group does not substantially affect the Cd(1)–O(6) distance, which is only 0.023 Å longer than the Cd(1)–O(1) one. The strongest Cd-donor interactions are provided by the nitrogen atoms of the pyridine units, the Cd(1)–N(2) and Cd(1)–N(3) distances being 0.15–0.21 Å shorter than the remaining bond lengths of the metal coordination environment. The metal–donor distances are substantially shorter than those observed for the corresponding complex of **bp12c4**, in which the metal ion is eight-coordinate.[15] The distances between the Cd^{II} ion and the donor atoms of the pendant arms are intermediate between those observed in the bis- and tris(dipicolinate) complexes.[25] The distance between the Cd^{II} ion and the oxygen atom of the crown moiety O(5) is ca. 0.09 Å longer than those observed in Cd^{II} complexes of 12-crown-4,[26] but similar to those observed in complexes derived from 15-crown-5[27] or diaza-15-crown-5.[28] However, the Cd–O(5) distance is clearly shorter than those observed in complexes derived from 18-crown-6[26] or diaza-18-crown-6.[29]

Table 4. Bond lengths [Å] and angles [°] of the metal coordination environment in [Cd(**Hbp15c5**)]$^+$; see Figure 4 for labeling.

Cd(1)–N(4)	2.277(7)	Cd(1)–O(6)	2.45(1)
Cd(1)–N(1)	2.298(7)	Cd(1)–O(5)	2.48(1)
Cd(1)–O(1)	2.43(1)	Cd(1)–N(3)	2.486(7)
Cd(1)–N(2)	2.446(7)		
N(4)–Cd(1)–N(1)	130.6(2)	N(1)–Cd(1)–O(5)	75.9(3)
N(4)–Cd(1)–O(1)	80.6(3)	O(1)–Cd(1)–O(5)	84.5(4)
N(1)–Cd(1)–O(1)	70.8(3)	N(2)–Cd(1)–O(5)	73.5(3)
N(4)–Cd(1)–N(2)	136.1(2)	O(6)–Cd(1)–O(5)	148.0(4)
N(1)–Cd(1)–N(2)	71.8(2)	N(4)–Cd(1)–N(3)	72.3(2)
O(1)–Cd(1)–N(2)	140.2(3)	N(1)–Cd(1)–N(3)	136.7(3)
N(4)–Cd(1)–O(6)	68.7(3)	O(1)–Cd(1)–N(3)	80.1(3)
N(1)–Cd(1)–O(6)	73.0(3)	N(2)–Cd(1)–N(3)	120.3(2)
O(1)–Cd(1)–O(6)	92.1(4)	O(6)–Cd(1)–N(3)	141.0(3)
N(2)–Cd(1)–O(6)	89.8(3)	O(5)–Cd(1)–N(3)	69.8(3)
N(4)–Cd(1)–O(5)	141.0(3)		

To obtain information on the solution structure of the [M(**bp15c5**)] complexes (M = Ca, Zn, Cd, or Pb), as well as to investigate the possible stereochemical activity of the Pb^{II} lone pair, these systems were characterized by means of DFT calculations (B3LYP model). On the grounds of our previous experience,[15,22,29] in these calculations the 6-31G(d) basis set was used for the ligand atoms, while for the metals the effective core potential of Wadt and Hay (Los Alamos ECP) included in the LanL2DZ basis set was applied.

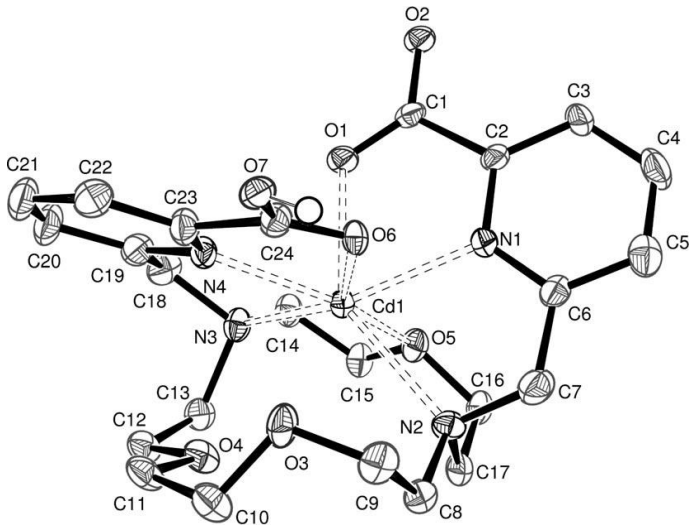

Figure 4. X-ray crystal structure of [Cd(**Hbp15c5**)]$^{+}$ in [Cd(**Hbp15c5**)](ClO_4)·0.5H_2O with atom labeling; hydrogen atoms, except that of the protonated picolinate group, are omitted for simplicity. The ORTEP plot is drawn at the 50 % probability level.

A *syn* conformation of the ligand in [M(**bp15c5**)] complexes (M = Ca, Zn, Cd, or Pb) implies the occurrence of two helicities: one associated with the layout of the picolinate pendant arms (absolute configuration Δ or Λ), and the other to the four five-membered chelate rings formed by the binding of the crown moiety (each of them showing absolute configuration δ or λ).[30,31] A detailed analysis of the coordinative properties of the **bp15c5** ligand indicates that there are up to 64 possible conformations (32 enantiomeric pairs of diastereoisomers) of the complexes of this ligand combining different helicities of the pendant arms and the five-membered rings formed upon coordination of the crown moiety. Thus, 32 diastereoisomeric forms of the complexes were first fully optimized at the HF/LanL2DZ/6-31G(d) level. The eight most stable conformations for each complex were then fully optimized at the B3LYP/LanL2DZ/6-31G(d) level. Full geometry optimization of each conformation performed in vacuo was followed by single-point energy calculations in aqueous solution. The minimum energy conformations obtained for the different [M(**bp15c5**)] complexes (M = Ca, Zn, Cd, or Pb) are shown in Figure **5**. The optimized Cartesian coordinates obtained for the minimum energy conformations of each complex are given as Supporting Information, while the optimized bond lengths of the metal coordination environments are given in Table **5**.

Table 5. Bond lengths [Å] of the metal coordination environments obtained for the minimum energy conformations of [M(**bp15c5**)] complexes at the B3LYP/LanL2DZ/6-31G(d) level.

M(1)–N(4)	2.148	2.378	2.685	2.628
M(1)–N(1)	2.260	2.359	2.492	2.507
M(1)–O(1)	2.023	2.265	2.297	2.359
M(1)–N(2)	[a]	2.872	2.897	2.812
M(1)–O(6)	2.066	2.296	2.255	2.415
M(1)–O(5)	2.261	2.489	3.000	3.502
M(1)–N(3)	2.636	2.797	[a]	2.916
M(1)–O(3)	[a]	[a]	[a]	2.900
M(1)–O(4)	[a]	[a]	[a]	3.065

[a] The M–donor distance is too long to be considered as a bond length.

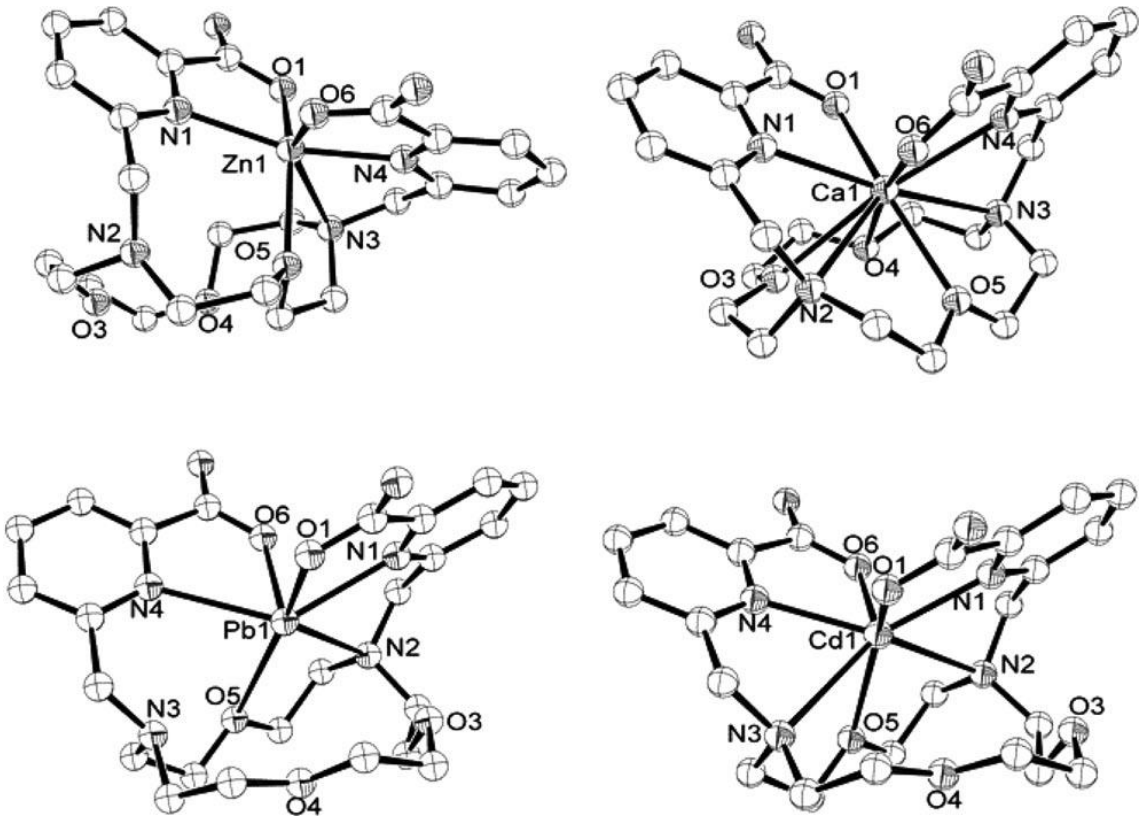

Figure 5. Minimum energy conformations of the [M(**bp15c5**)] complexes optimized at the B3LYP/LanL2DZ/6-31G(d) level.

Among the 32 conformations investigated in the case of the [Cd(**bp15c5**)] complex our DFT calculations provide a lowest energy conformation that is very similar to that observed in the solid state for $[Cd(\mathbf{Hbp15c5})]^{+}$ (see above), in which the metal ion is seven-coordinate by the donor atoms of the two picolinate pendants [N(1), O(1), N(4), and O(6)], the two pivotal nitrogen atoms [N(2) and N(3)] and one of the oxygen atoms of the crown moiety [O(5)]. This gives us confidence in the predictions of the computational procedure used for conformational analysis, as the x-ray crystal structure was not used as input geometry in these calculations.

For the [Zn(**bp15c5**)] system, our calculations provide a minimum energy conformation in which the metal ion is bound only to six of the nine donor atoms of the ligand. The metal ion is placed at one end of the macrocyclic cavity, being directly bound only to one of the pivotal nitrogen atoms [N(3)] and one of the oxygen atoms of the crown moiety [O(5)]. This is in contrast to the situation observed for the [Zn(**bp12c4**)] analogue, in which the metal ion is coordinated by the eight donor atoms of the ligand. Thus, the dramatic drop of complex stability in [Zn(**bp15c5**)] compared to [Zn(**bp12c4**)] (Table **2**) may be attributed to the so called *dislocation discrimination*.[32] Dislocation discrimination is associated with a sudden change in coordination behavior of a particular metal ion along a series of closely related macrocyclic ligands. In principle, a dislocation will occur when the gradation of ligand properties along the series results in a sudden destabilization of one complex structure relative to a second. This behavior is not observed however for Ca^{II}, with both **bp12c4** and **bp15c5** providing complexes with very similar stabilities. This is in line with the minimum energy conformation obtained for [Ca(**bp15c5**)], in which the metal ion is directly bound to eight of the nine donor atoms of the ligand, the ninth donor atom [O(4)] providing a weak interaction.

In the case of the Cd^{II} complex a slight decrease of the complex stability is observed on going from **bp12c4** to **bp15c5**. Both our DFT calculations and the X-ray crystal structure show that for this

complex two of the donor atoms of the ligand are not coordinated to the metal ion, and therefore a lower stability is expected for the **bp15c5** complex when compared to the **bp12c4** analogue.[15] However, in the [Cd(**bp15c5**)] complex the metal ion is endocyclicly coordinated by the ligand, while for the Zn^{II} analogue the metal ion is placed outside the macrocyclic cavity. Indeed, according to our DFT calculations the Zn^{II} ion is only bound to one of the oxygen atoms of the crown moiety [O(5)], while a weak interaction is observed between Zn^{II} and one of the pivotal nitrogen atoms [N(3), see Table **5**]. As a consequence a very important drop of complex stability is observed for Zn^{II} upon increasing the macrocyclic ring size on going from **bp12c4** to **bp5c5**, while only a slight decrease of complex stability is observed for the Cd^{II} analogue.

Finally, our DFT calculations on the [Pb(**bp15c5**)] system provide a minimum energy conformation in which the metal ion is asymmetrically coordinated to the macrocyclic ligand. The donor atoms of the pendant arms provide the strongest binding to the metal ion, which is also bound to one of the pivotal nitrogen atoms [N(2)]. One of the oxygen atoms of the macrocycle [O(5)] provides a weak interaction with the metal ion, while the other two oxygen atoms of the crown moiety and the second pivotal nitrogen atom remain uncoordinated [Pb(1)–O(3) 3.31 Å; Pb(1)–O(4) 3.39 Å, Pb(1)–N(3) 3.30 Å]. As can be seen in Figure **5** the disposition of the donor atoms of the ligand around the Pb^{II} ion results in an identifiable void. This is typical of the so-called hemidirected compounds, in which the lone pair of electrons causes a nonspherical charge distribution around the Pb^{II} cation.[33,34] Indeed, an analysis of the natural bond orbitals (NBOs) shows that the Pb^{II} lone pair possesses a predominant 6*s* character, but it is polarized by a substantial 6*p* contribution: *s*[97.21 %]*p*[2.79 %]. Similar *p* contributions (1.89–4.39 %) have been calculated for different hemidirected four-coordinate Pb^{II} complexes with neutral ligands, while *p* contributions in the range 2.62–15.72 % have been calculated for hemidirected four-coordinate Pb^{II} complexes with anionic ligands.[33] A hemidirected geometry has also been observed in the solid state for the [Pb(**bp12c4**)] analogue.[15]

The stability of the [Pb(**bp15c5**)] complex is somewhat higher than that of the **bp12c4** analogue (see Tables **1** and **2**), while our DFT calculations provide a minimum energy conformation for the [Pb(**bp15c5**)] complex that shows a poor complementarity between the donor atoms offered by the ligand and the metal ion. This effect is attributed to the stereochemical activity of the Pb^{II} lone pair. Indeed, Pb^{II} would have a preference, according to the VSEPR theory, to adopt a linear coordination geometry where one of the coordination sites is occupied by the lone pair. Thus, higher stability should be expected for ligands that occupy only the site opposite to the lone pair.[35] For instance a higher stability has been observed for the Pb^{II} complex of a dipodal picolinate ligand in comparison to the tripodal analogue.[34b] In the complex of the dipodal ligand the donor atoms occupy only a quarter of the coordination sphere, reducing the steric interaction between the lead lone pair and the ligand, and therefore leading to increased stability.[34b] A similar effect is probably responsible for the increased stability of the Pb^{II} complex of **bp15c5** when compared to the **bp14c4** analogue, the larger macrocyclic cavity of **bp15c5** reducing the steric interaction between the Pb^{II} lone pair and the ligand.

Conclusions

The nonadentate ligand **bp15c5** forms thermodynamically stable Ca^{II}, Zn^{II}, Cd^{II}, and Pb^{II} complexes in aqueous solution. The stability constants vary in the following order: $Pb^{II} > Cd^{II} >> Zn^{II} > Ca^{II}$. As a consequence, the complexes of **bp15c5** present important Pb^{II}/Ca^{II} and Pb^{II}/Zn^{II} selectivities, an interesting property that might be useful for the elimination of Pb^{II} from living bodies.[36] The stability of the Ca^{II}, Cd^{II}, and Pb^{II} complexes of **bp15c5** is relatively similar to that observed for the **bp12c4** analogue. However, increasing the macrocyclic ring size from **bp12c4** to **bp15c5** results in a dramatic drop of complex stability for Zn^{II}, which is attributed to the so-called dislocation discrimination.

Experimental section

Solvents and starting materials: Methyl 6-(chloromethyl)pyridine-2-carboxylate was prepared following the literature method.[37] All other chemicals were purchased from commercial sources and used without further purification, unless otherwise stated.

Caution! *Although we have experienced no difficulties with the perchlorate salts, these should be regarded as potentially explosive and handled with great care.*[38]

N,*N*′-Bis[(6-carboxy-2-pyridyl)methyl]-1,10-diaza-15-crown-5(H_2bp15c5·3HCl·3H_2O): Methyl 6-(chloromethyl)pyridine-2-carboxylate (1.72 g, 9.27 mmol) and Na_2CO_3 (4.90 g, 46.22 mmol) were added to a solution of 1,10-diaza-15-crown-5 (1.01 g, 4.63 mmol) in acetonitrile (60 mL). The mixture was heated to reflux with stirring for a period of 48 h, and then excess Na_2CO_3 was filtered off. The filtrate was concentrated to dryness and the yellow residue partitioned between equal volumes (200 mL) of H_2O and CH_3Cl. The organic phase was separated, dried with $MgSO_4$, filtered, and the solvents evaporated to dryness to give a yellow oil. This was purified on a silica column, eluting with acetonitrile/water/satd. aq. KNO_3 (14:2:1). The fractions containing the product (R_f = 0.71) were collected, and the resultant solution concentrated to dryness. The residue was dissolved in CH_2Cl_2 (30 mL), the solution was dried with anhydrous Na_2SO_4, and then filtered. The solvent was evaporated, the residue was dissolved in 6 M HCl (11 mL) and the solution heated to reflux for 48 h. After cooling to room temperature the solvent was removed to give 1.18 g of a hygroscopic brown solid (yield 39 %); m.p. 58–60 °C. $C_{24}H_{32}N_4O_7$·3HCl·3H_2O (650.96): calcd. C 41.87, H 6.15, N 8.14; found C 40.04, H 5.78, N 8.14. MS (FAB, 3-nba): *m*/*z* = 489 $[C_{24}H_{33}N_4O_7]^+$. IR (ATR): $\tilde{\nu}$ = 1721 (C=O), 1634 (C=N), 1593 (C=C), 1124 (C–O) cm^{-1}. ^{1}H NMR (D_2O, 500 MHz, 25 °C, TMS, pD = 7.0): δ = 7.95 (m, 2 H, py), 7.84 (d, ^3J = 7.6 Hz, 2 H, py), 7.58 (d, ^3J = 7.2 Hz, 2 H, py), 4.59 (s, 4 H, -CH_2-py), 3.81 (m, 4 H, O-CH_2-CH_2-O), 3.62 (m, 8 H, N-CH_2-CH_2-O), 3.54 (m, 8 H, N-CH_2-CH_2-O) ppm. ^{13}C NMR (D_2O, 125.8 MHz, 25 °C, TMS, pD = 7.0): δ = 174.2, 155.9, 150.7, 140.9, 127.4, 125.3, 71.3, 65.1, 64.8, 59.9, 54.8 ppm.

Physical methods: ^{1}H and ^{13}C NMR spectra were recorded at 25 °C with Bruker Avance 300 and Bruker Avance 500 MHz spectrometers. For measurements in D_2O, *tert*-butyl alcohol was used as an internal standard with the methyl signal calibrated at δ = 1.2 (^{1}H) and 31.2 ppm (^{13}C). Spectral assignments were based in part on two-dimensional COSY, HMQC, and HMBC experiments. Ligand protonation constants and stability constants with Zn^{II}, Cd^{II}, Pb^{II}, and Ca^{II} were determined by pH-potentiometric titration at 25 °C in 0.1 M KNO_3. The samples (10 mL) were stirred while a constant Ar flow was bubbled through the solutions. The titrations were carried out adding a standardized KOH solution with a Metrohm Dosimat 794 automatic burette. KOH was standardized by potentiometric titration against potassium hydrogen phthalate. A glass electrode filled with 3 M KCl was used to measure pH. The stock solutions of MCl_2 (M = Ca, Zn, or Cd) and $Pb(NO_3)_2$ were prepared by dilution of the appropriate standards (Aldrich). The pH of the titration mixture was adjusted by addition of a known volume of standard HNO_3. The exact amount of acid present in the standard solutions was determined by pH measurement. **H_2bp15c5** was checked for purity by NMR and elemental analysis before titration. The ligand and metal–ligand (1:1) solutions were titrated over the pH range 2.0 < pH < 11.0. In the case of the metal–ligand (1:1) solutions reverse titrations were performed to check the reversibility of the system. Reverse titrations were carried out adding a standardized HNO_3 solution; the pH of the titration mixture was adjusted by addition of a known volume of standard KOH. The protonation and stability constants were calculated from simultaneous fits of three independent titrations with the program HYPERQUAD.[39] The errors given correspond to one standard deviation.

Computational methods: All calculations were performed employing hybrid DFT with the B3LYP exchange-correlation functional,[40,41] and the Gaussian 03 package (Revision C.01).[42] Full geometry optimizations of the [M(**bp15c5**)] (M = Ca, Zn, Cd, or Pb) systems were performed in vacuo by using the standard 6–31G(d) basis set for the ligand atoms and the LanL2DZ valence and effective core potential functions for the

metals.[43] The stationary points found on the potential energy surfaces as a result of the geometry optimizations have been tested to represent energy minima rather than saddle points via frequency analysis. In aqueous solution relative free energies of the different conformations of the complexes were calculated from solvated single-point energy calculations on the geometries optimized in vacuo. In these calculations solvent effects were evaluated by using the polarizable continuum model (PCM). In particular, we used the C–PCM variant[44] that employs conductor rather than dielectric boundary conditions. The solute cavity is built as an envelope of spheres centered on atoms or atomic groups with appropriate radii. Calculations were performed using an average area of 0.2 $Å^2$ for all the finite elements (tesserae) used to build the solute cavities. Free energies include both electrostatic and nonelectrostatic contributions and nonpotential energy terms (that is, zero point energies and thermal terms) obtained from frequency analysis performed in vacuo. The wave functions of the [Pb(**bp15c5**)] complex were analyzed by natural bond orbital analyses, involving natural atomic orbital (NAO) populations and natural bond orbitals (NBO).[45,46]

X-ray crystal structure: Single crystals of formula [Cd(**Hbp15c5**)](ClO_4)·0.5H_2O were obtained by reacting **H_2bp15c5**·3HCl·3H_2O (0.315 g, 0.296 mmol), Cd(ClO_4)$_2$ (0.100 g, 0.321 mmol), and triethylamine (0.150 g, 1.48 mmol) in 2-propanol (5 mL). The mixture was refluxed for 30 min and filtered while hot. Slow evaporation of the filtrate at room temperature provided colorless single crystals. Three-dimensional X-ray data were collected with a Bruker X8 APEXII CCD. Data were corrected for Lorentz and polarization effects and for absorption by semiempirical methods[47] based on symmetry-equivalent reflections. Complex scattering factors were taken from the program SHELX97[48] running under the WinGX program system[49] as implemented on a Pentium® computer. The structure was solved by the Patterson method (DIRDIF2008[50]) and was refined[48] by full-matrix least-squares on F^2. All hydrogen atoms were included in calculated positions and refined in riding mode, except those of the water molecule that were located in a difference electron-density map and all the distances between atoms fixed; 722 least-square restraints had to be imposed to fix the positional disorder for the perchlorate group and the crown chain. The crystal of the cadmium complex is heavily disordered with a perchlorate group disordered in at least three positions with occupation factors of 0.496(8), 0.207(16), and 0.296(16); the crown chain was disordered as well with an occupation factor of 0.527(5) for the most occupied positions. Finally, refinement converged with anisotropic displacement parameters for all non-hydrogen atoms. Crystal data: $C_{24}H_{32}CdClN_4O_{11.50}$, F_W = 708.39. Monoclinic, space group $P12_1/n1$, a = 9.477(3), b = 29.738(7), c = 9.750(3) Å, β = 94.714(16)°, V = 2738.5(14) $Å^3$, T = 100.0(2) K, $2\theta_{max}$ = 26.7°, Z = 4, $\rho_{calcd.}$ = 1.718 g cm^{-3}, μ = 0.965 mm^{-1}, $F(000)$ = 1444, 6867 reflections collected, 5865 unique [R_{int} = 0.0554], final R indexes [$I > 2\sigma(I)$] R_1 = 0.0978, wR_2 = 0.2024, final R indexes [all data] R_1 = 0.1127, wR_2 = 0.2052, $\rho_{max/min}$ = –2.718/0.188 e $Å^{-3}$.

CCDC-CCDC-758195 http://www.ccdc.cam.ac.uk/cgi-bin/catreq.cgi (for Cd(**Hbp15c5**)](ClO_4)·0.5H_2O) contains the supplementary crystallographic data for this paper. These data can be obtained free of charge from the Cambridge Crystallographic Data Centre via www.ccdc.cam.ac.uk/data_request/cif.

Supporting Information

Figures S1 and S2 showing variable temperature ^{1}H NMR spectra of [Ca(**bp15c5**)] and [Pb(**bp15c5**)] complexes, and in vacuo optimized Cartesian coordinates [Å] for the [M(**bp15c5**)] complexes (M = Zn, Cd, Pb, or Ca). See also the footnote on the last page of this article.

Acknowledgements

The authors thank Xunta de Galicia (PGIDIT06TAM10301PR and INCITE09E1R103013ES) for generous financial support. The authors are indebted to Centro de Supercomputación de Galicia (CESGA) for

providing the computer facilities. The authors gratefully acknowledge Dr. Bruno Dacunha Marinho for useful discussions and help with the refinement of the crystal structure.

References

[1] a) A. Roca-Sabio, M. Mato-Iglesias, D. Esteban-Gomez, E. Toth, A. de Blas, C. Platas-Iglesias, T. Rodriguez-Blas, *J. Am. Chem. Soc*. **2009**, *131*, 3331–3341; b) J. S. Bradshaw, R. M. Izatt, *Acc. Chem. Res*. **1997**, *30*, 338–345; c) Y. Nakatsuji, T. Nakamura, M. Yonetani, H. Yuya, M. Okahara, *J. Am. Chem. Soc.* **1988**, *110*, 531–538; d) G. W. Gokel, *Chem. Soc. Rev*. **1992**, *21*, 39–47.

[2] a) B. S. Creaven, D. F. Donlon, J. McGinley, *Coord. Chem. Rev*. **2009**, *253*, 893–962; b) C. Redshaw, *Coord. Chem. Rev*. **2003**, *244*, 45–70; c) A. Ikeda, S. Shinkai, *Chem. Rev*. **1997**, *97*, 1713–1734.

[3] a) C. J. Pederson, J.-M. Lehn, D. J. Cram, *Resonance* **2001**, *6*, 71–79; b) M. Formica, V. Fusi, M. Micheloni, R. Pontellini, P. Romani, *Coord. Chem. Rev*. **1999**, *184*, 347–363; c) X.-X. Zhang, R. M. Izatt, J. S. Bradshaw, K. E. Krakowiak, *Coord. Chem. Rev*. **1998**, *174*, 179–189.

[4] a) R. D. Hancock, A. E. Martell, *Chem. Rev*. **1989**, *89*, 1875–1914; b) R. D. Hancock, A. E. Martell, *Supramol. Chem*. **1996**, *6*, 401–407; c) B. P. Hay, R. D. Hancock, *Coord. Chem. Rev*. **2001**, *212*, 61–78.

[5] R. D. Hancock, H. Maumela, A. S. de Sousa, *Coord. Chem. Rev*. **1996**, *148*, 315–317.

[6] Y. Inoue, G. W. Gokel (Eds.), *Cation Binding by Macrocycles. Complexation of Cationic Species by Crown Ethers*, Marcel Dekker, New York, **1990**.

[7] a) R. M. Izatt, K. Pawlak, J. S. Bradshaw, R. L. Bruening, *Chem. Rev*. **1991**, *91*, 1721–1785; b) R. M. Izatt, J. S. Bradshaw, K. Pawlak, R. L. Bruening, B. J. Tarbet, *Chem. Rev*. **1992**, *92*, 1261–1354; c) G. W. Gokel, *Chem. Soc. Rev*. **1992**, *21*, 39–47; d) R. M. Izatt, K. Pawlak, J. S. Bradshaw, *Chem. Rev*. **1995**, *95*, 2529–2586.

[8] R. M. Harrison, D. R. H. Laxen, *Lead Pollution*, Chapman and Hall, London, **1981**.

[9] G. F. Nordberg, *BioMetals* **2004**, *17*, 485–489.

[10] R. A. Goyer, in: *Handbook on Toxicity of Inorganic Compounds* (Eds.: H. G. Seiler, A. Sigel, H. Sigel), Marcel Dekker, New York, **1988**, pp. 359–382.

[11] a) H. Sigel, C. P. Da Costa, R. B. Martin, *Coord. Chem. Rev*. **2001**, *219–221*, 435–461; b) H. Sigel, B. E. Fischer, E. Farkas, *Inorg. Chem*. **1983**, *22*, 925–934; c) H. A. Tajimir-Riahi, M. Langlais, R. Savoie, *Nucleic Acids Res*. **1988**, *16*, 751–762; d) G. Kazantis, in: *Poisoning, Diagnosis and Treatment* (Eds.: J. A. Vale, T. J. Meredith), Update Books, London, **1981**, pp. 171–175; e) D. Baltrop, in: *Poisoning, Diagnosis and Treatment* (Eds.: J. A. Vale, T. J. Meredith), Update Books, London, **1981**, pp. 178–185.

[12] a) C. P. Da Costa, H. Rigel, *Inorg. Chem*. **2000**, *39*, 5985–5993; b) R. B. Martin, *Inorg. Chim. Acta* **1998**, *283*, 30–36; c) J. S. Magyar, T.-C. Weng, Ch. M. Stern, D. F. Dye, B. W. Rous, J. C. Payne, M. A. Bridgewater, B. Mijovilovich, G. Parkin, J. M. Zaleski, J. E. Penner-Hahn, H. A. Godwin, *J. Am. Chem. Soc.* **2005**, *127*, 9495–9505.

[13] a) B. P. Lanphear, R. Hornung, J. Khoury, K. Yolton, P. Baghurst, D. C. Bellinger, R. L. Canfield, K. N. Dietrich, R. Bornschein, T. Greene, S. J. Rothenberg, H. L. Needleman, L. Schnaas, G.

Wasserman, J. Graziano, R. Roberts, *Environ. Health Perspect*. **2005**, *113*, 894–899; b) C. Castellino, P. Castellino, N. Sannolo (Eds.), *Inorganic Lead Exposure: Metabolism and Intoxication*, Lewis, Boca Raton, FL, **1994**.

[14] F. M. R. Bulmer, H. E. Rothwell, E. R. Frankish, *Can. Pub. Health J.* **1938**, *29*, 19–26.

[15] R. Ferreiros-Martínez, D. Esteban-Gómez, A. de Blas, C. Platas-Iglesias, T. Rodríguez-Blas, *Inorg. Chem.* **2009**, *48*, 11821–11831.

[16] a) M. Mato-Iglesias, A. Roca-Sabio, Z. Palinkas, D. Esteban-Gomez, C. Platas-Iglesias, E. Toth, A. de Blas, T. Rodriguez-Blas, *Inorg. Chem*. **2008**, *47*, 7840–7851; b) Z. Palinkas, A. Roca-Sabio, M. Mato-Iglesias, D. Esteban-Gomez, C. Platas-Iglesias, A. de Blas, T. Rodriguez-Blas, E. Toth, *Inorg. Chem*. **2009**, *48*, 8878–8889.

[17] C. A. Chang, V. O. Ochaya, *Inorg. Chem*. **1986**, *25*, 355–358.

[18] M. T. S. Amorim, R. Delgado, J. J. R. Frausto da Silva, *Polyhedron* **1992**, *11*, 1891–1899.

[19] N. Chatterton, C. Gateau, M. Mazzanti, J. Pecaut, A. Borel, L. Helm, A. E. Merbach, *Dalton Trans*. **2005**, 1129–1135.

[20] J. Costa, E. Toth, L. Helm, A. E. Merbach, *Inorg. Chem*. **2005**, *44*, 4747–4755.

[21] M. Mato-Iglesias, E. Balogh, C. Platas-Iglesias, E. Toth, A. de Blas, T. Rodríguez-Blas, *Dalton Trans*. **2006**, 5404–5415.

[22] a) R. Ferreiros-Martinez, D. Esteban-Gomez, C. Platas-Iglesias, A. de Blas, T. Rodriguez-Blas, *Dalton Trans*. **2008**, 5754–5765; b) R. Ferreirós-Martínez, D. Esteban-Gómez, C. Platas-Iglesias, A. de Blas, T. Rodríguez-Blas, *Inorg. Chem*. **2009**, *48*, 10976–10987.

[23] C. J. Sunderland, M. Botta, S. Aime, K. N. Raymond, *Inorg. Chem*. **2001**, *40*, 6746–6756.

[24] a) L. Vaiana, M. Regueiro-Figueroa, M. Mato-Iglesias, C. Platas-Iglesias, D. Esteban-Gómez, A. de Blas, T. Rodríguez-Blas, *Inorg. Chem*. **2007**, *46*, 8271–8282; b) M. González-Lorenzo, C. Platas-Iglesias, F. Avecilla, C. F. G. C. Geraldes, D. Imbert, J.-C. G. Bünzli, A. de Blas, T. Rodríguez-Blas, *Inorg. Chem*. **2003**, *42*, 6946–6954.

[25] a) H. Aghabozorg, Z. Aghajani, M. A. Sharif, *Acta Crystallogr., Sect. E* **2006**, *62*, m1930–m1932; b) A.-Y. Fu, D.-Q. Wang, A.-Z. Liu, *Acta Crystallogr., Sect. E* **2004**, *60*, m1372–m1373.

[26] a) H. Zhang, X. Wang, H. Zhu, W. Xiao, B. K. Teo, *J. Am. Chem. Soc*. **1997**, *119*, 5463–5464; b) P. C. Junk, M. K. Smith, J. W. Steed, *Polyhedron* **2001**, *20*, 2979–2988.

[27] A. H. Bond, R. D. Rogers, *J. Chem. Crystallogr*. **1998**, *28*, 521–527.

[28] D. Esteban, D. Bañobre, A. de Blas, T. Rodríguez-Blas, R. Bastida, A. Macías, A. Rodríguez, D. E. Fenton, H. Adams, J. Mahía, *Eur. J. Inorg. Chem*. **2000**, 1445–1456.

[29] M. Regueiro-Figueroa, D. Esteban-Gomez, C. Platas-Iglesias, A. de Blas, T. Rodríguez-Blas, *Eur. J. Inorg. Chem.* **2007**, 2198–2207.

[30] E. J. Corey, J. C. Bailar Jr., *J. Am. Chem. Soc*. **1959**, *81*, 2620–2629.

[31] J. K. Beattie, *Acc. Chem. Res*. **1971**, *4*, 253–259.

[32] K. R. Adam, K. P. Dancey, A. J. Leong, L. F. Lindoy, B. J. McCool, M. McPartlin, P. A. Tasker, *J. Am. Chem. Soc.* **1988**, *110*, 8471–8477.

[33] L. Shimoni-Livny, J. P. Glusker, C. W. Bock, *Inorg. Chem*. **1998**, *37*, 1853–1867.

[34] a) D. Esteban-Gómez, C. Platas-Iglesias, T. Enríquez-Pérez, F. Avecilla, A. de Blas, T. Rodríguez-Blas, *Inorg. Chem*. **2006**, *45*, 5407–5416; b) A. Pellissier, Y. Bretonniere, N. Chatterton, J. Pecaut, P. Delangle, M. Mazzanti, *Inorg. Chem.* **2007**, *46*, 3714–3725.

[35] R. Luckay, I. Cukrowski, J. Mashishi, J. H. Reibenspies, A. H. Bond, R. D. Rogers, R. D. Hancock, *J. Chem. Soc., Dalton Trans*. **1997**, 901–908.

[36] a) O. Andersen, *Chem. Rev*. **1999**, *99*, 2683–2710; b) M. Blanusa, V. M. Varnai, M. Piasek, K. Kostial, *Curr. Med. Chem*. **2005**, *12*, 2771–2794.

[37] E. J. T. Chrystal, L. Couper, D. J. Robins, *Tetrahedron* **1995**, *51*, 10241–10252.

[38] W. C. Wolsey, *J. Chem. Educ*. **1973**, *50*, A335–A337.

[39] P. Gans, A. Sabatini, A. Vacca, *Talanta* **1996**, *43*, 1739–1753.

[40] A. D. Becke, *J. Chem. Phys*. **1993**, *98*, 5648–5652.

[41] C. Lee, W. Yang, R. G. Parr, *Phys. Rev. B* **1988**, *37*, 785–789.

[42] *Gaussian 03*, Revision C.01, M. J. Frisch, G. W. Trucks, H. B. Schlegel, G. E. Scuseria, M. A. Robb, J. R. Cheeseman, J. A. Montgomery Jr., T. Vreven, K. N. Kudin, J. C. Burant, J. M. Millam, S. S. Iyengar, J. Tomasi, V. Barone, B. Mennucci, M. Cossi, G. Scalmani, N. Rega, G. A. Petersson, H. Nakatsuji, M. Hada, M. Ehara, K. Toyota, R. Fukuda, J. Hasegawa, M. Ishida, T. Nakajima, Y. Honda, O. Kitao, H. Nakai, M. Klene, X. Li, J. E. Knox, H. P. Hratchian, J. B. Cross, V. Bakken, C. Adamo, J. Jaramillo, R. Gomperts, R. E. Stratmann, O. Yazyev, A. J. Austin, R. Cammi, C. Pomelli, J. W. Ochterski, P. Y. Ayala, K. Morokuma, G. A. Voth, P. Salvador, J. J. Dannenberg, V. G. Zakrzewski, S. Dapprich, A. D. Daniels, M. C. Strain, O. Farkas, D. K. Malick, A. D. Rabuck, K. Raghavachari, J. B. Foresman, J. V. Ortiz, Q. Cui, A. G. Baboul, S. Clifford, J. Cioslowski, B. B. Stefanov, G. Liu, A. Liashenko, P. Piskorz, I. Komaromi, R. L. Martin, D. J. Fox, T. Keith, M. A. Al-Laham, C. Y. Peng, A. Nanayakkara, M. Challacombe, P. M. W. Gill, B. Johnson, W. Chen, M. W. Wong, C. Gonzalez, J. A. Pople, Gaussian, Inc., Wallingford CT, **2004**.

[43] a) P. J. Hay, W. R. Wadt, *J. Chem. Phys*. **1985**, *82*, 270–283; b) P. J. Hay, W. R. Wadt, *J. Chem. Phys.* **1985**, *82*, 284–298; c) P. J. Hay, W. R. Wadt, *J. Chem. Phys*. **1985**, *82*, 299–310.

[44] V. Barone, M. Cossi, *J. Phys. Chem. A* **1998**, *102*, 1995–2001.

[45] E. D. Glendening, A. E. Reed, J. E. Carpenter, F. Weinhold, *NBO version 3.1*.

[46] A. E. Reed, L. A. Curtiss, F. Weinhold, *Chem. Rev*. **1988**, *88*, 899–926.

[47] *SABADS*, Bruker-AXS Version **2004/1**, Bruker AXS Inc., Madison, Wisconsin, USA.

[48] SHELX, G. M. Sheldrick, *Acta Crystallogr., Sect. A* **2008**, *64*, 112–122.

[49] WinGX MS-Windows system of programs for solving, refining and analyzing single-crystal X-ray diffraction data for small molecules, L. J. Farrugia, *J. Appl. Crystallogr*. **1999**, *32*, 837–838.

[50] *DIRDIF-2008*, P. T. Beurskens, G. Beurskens, R. Gelder, J. M. M. Smits, S. Garcia-Granda, R. O. Gould, Crystallography Laboratory, Radbound University Nijmegen, Toernooiveld 1, 6526 ED Nijmegen, The Netherlands, **2008**.

[i] Supporting information for this article is available online: https://doi.org/10.1002/ejic.200901219.